CONTROL OF TRANSFORMERLESS INVERTER FOR A PV SYSTEM USING FUZZY LOGIC AND FRACTIONAL CONTROLLER

A PROJECT REPORT

submitted by

RISANA S
(Reg. No. TKM20EEII15)

to

the APJ Abdul Kalam Technological University
in partial fulfillment of the requirements for the award of the Degree

of

Master of Technology
in
Electrical and Electronics Engineering

with specialisation in

Industrial Instrumentation and Control

Department of Electrical and Electronics Engineering
TKM College of Engineering
Kollam - 691 005
KERALA

SEPT 2022

DECLARATION

I undersigned hereby declare that the project report entitled "**Control of Transformerless Inverter for a PV System using Fuzzy Logic and Fractional Controller** ", submitted for partial fulfillment of the requirements for the award of degree of Master of Technology in Electrical and Electronics Engineering with specialisation in Industrial Instrumentation and Control, of the APJ Abdul Kalam Technological University, Kerala is a bonafide work done by me under supervision of *Prof. Irfan Habeeb*, Assistant Professor, Department of Electrical and Electronics Engineering. This submission represents my ideas in my own words and where ideas or words of others have been included. I have adequately and accurately cited and referenced the original sources. I also declare that I have adhered to ethics of academic honesty and integrity and have not misrepresented or fabricated any data or idea or fact or source in my submission. I understand that any violation of the above will be a cause for disciplinary action by the institute and/or the University and can also evoke penal action from the sources which have thus not been properly cited or from whom proper permission has not been obtained. This report has not been previously formed the basis for the award of any degree, diploma or similar title of any other University.

Kollam
Sept 15, 2022

RISANA S

DEPARTMENT OF ELECTRICAL AND ELECTRONICS ENGINEERING

TKM COLLEGE OF ENGINEERING

KOLLAM - 691 005

CERTIFICATE

This is to certify that the report entitled " **Control of Transformerless Inverter for a PV System using Fuzzy Logic and Fractional Controller** " submitted by **RISANA S , (Reg. No. TKM20EEII15)** of fourth semester to the APJ Abdul Kalam Technological University in partial fulfillment of the requirements for the award of the Degree of Master of Technology in Electrical and Electronics Engineering with specialisation in Industrial Instrumentation and Control, is a bonafide record of the project work done by her under our guidance and supervision. This report in any form has not been submitted to any other University or Institute for any purpose.

Prof. Irfan Habeeb
Project Supervisor
Assistant Professor
Department of EEE
TKM College of Engineering

Prof. Sumayya Jaleel
Project Coordinator
Assistant Professor
Department of EEE
TKM College of Engineering

Prof. Shanavas T N
PG Coordinator
Associate Professor
Department of EEE
TKM College of Engineering

Dr. Sabeena Beevi K
Head of the Department
Associate Professor
Department of EEE
TKM College of Engineering

Acknowledgement

A lot of effort and hard work has been put into this project in course of its presentation. However, it would not have been possible without the kind support and help of many individuals and other sources. I would like to extend my sincere thanks to all of them. I take this opportunity to express my deep sense of gratitude and sincere thanks to all who helped me to complete this project report successfully.

I express my sincere thanks to *Dr. T A Shahul Hameed*, Principal, TKM College of Engineering for his encouragement in completion of my project.

I thank *Dr. Sabeena Beevi K*, Head of the Department, Department of Electrical and Electronics Engineering, *Dr. Imthias Ahamed T P*, Professor, Department of Electrical and Electronics Engineering and *Prof. Shanavas T N*, PG Coordinator, Department of Electrical and Electronics Engineering for their support and cooperation.

I am greatly thankful to my Project supervisor, *Prof Irfan Habeeb*, Assistant Professor, Department of Electrical and Electronics Engineering for their supervision, assistance and helpful suggestions.

I am deeply indebted to *Prof. Sumayya Jaleel*, Assistant Professor, Project Coordinator and *Prof. Amal A*, Assistant Professor, Department of Electrical and Electronics Engineering, for their excellent guidance, positive criticism and valuable comments.

Finally I thank my parents and friends near and dear ones who directly and indirectly contributed to the successful completion of my project.

RISANA S

Abstract

In the near future, the increase in fuel price and environmental constraints give more opportunities in favour of utilising renewable energy like solar. The integration of renewable energy source into a micro grid can cause impacts on grid operation. A new device called a smart inverter can aid in the integration of solar energy and other dispersed energy sources into the electrical grid. Here, a smart inverter with a single phase power supply is developed. In addition to supplying power to utility loads and local loads, SPV-SSI may inject power into the grid and store energy in lead acid batteries. The complete design of boost converter and bi-directional buck boost converter is presented here. More over fuzzy PI and fuzzy SMC is designed and fractional order PI controller is also used. Fuzzy PI and fuzzy SMC perform better and are more stable than traditionally tuned PI controllers, demonstrating the effectiveness of the system when utilising these controllers.

Contents

List of Tables

List of Figures

Abbreviations

BDC – DCBBC	Bidriectional DC DC Buck Boost Converter
DG	Distributed Generation
FLC	Fuzzy Logic Controller
FOPI	Fractional Order Proportional Integral
FPI	Fuzzy Proportional Integral
FSMC	Fuzzy Sliding Mode Controller
MPPT	Maximum Power Point Tracking
PI	Proportional Integral
PO	Perturb and Observe
PV	Photovoltaic
PWM	Pulse Width Modulation
SMC	Sliding Mode Controller
SPWM	Sinusoidal Pulse Width Modulation

Notations

A_{ref}	Sinusoidal Amplitude
f_{sw}	Switching Frequency
I_L	Inductor current
I_{max}	Current at Maximum Power
I_r	Irradiance
I_{SC}	Short Circuit Current
ϕ_{ref}	Phase Angle Reference
P_{max}	Maximum Power
P_{PU}	Active Power Component
Q_{PU}	Reactive Power Component
V_{max}	Voltage at Maximum Power
V_{OC}	Open Circuit Voltage

Chapter 1

INTRODUCTION

1.1 General Background

Due to the depletion of fossil fuel resources and ongoing worldwide environmental problems, the need to switch to sustainable energy sources is becoming increasingly essential [1]. Among the different renewable energy sources, the installation of solar photovoltaic (PV) energy is expanding quickly during the past few decades. As a result, the total SPV installation capacity is getting close to 405 GW. The installation capacity of PV (772 GW) is anticipated to surpass that of wind energy (735 GW) in 2020 [2][3]. Due to the increasing penetration of DG, advanced grid functions have recently been added to the requirements for distributed generation units that are connected to the power grid. These features are designed to sustain the electricity grid during erratic conditions and faults.

In order to control and integrate DG into the electricity grid, smart inverters (SIs) are crucial. In addition to its primary duty of converting DC power to AC power, it also performs numerous other tasks, such as voltage regulation, ramp-rate control, active power control, frequency control, and fault ride-through. Due to its promising characteristics of bi-directional energy flow competency, low-current harmonics, and high-power factor, single-phase voltage-SIs (SPV-SIs) are frequently employed in DGUs . Inverters that are connected to the grid have received a lot of attention in studies as a reliable way to inject PV-generated electricity. Inverter topologies, control strategies, and controller design are among the subjects discussed.

Numerous controllers are being investigated to control the steady-state and transient states performances of grid-connected PVs. These include the sliding mode controller (SMC), the

proportional-resonant (PR) controller, the deadbeat controller, the hysteresis controller, the repetitive controller, and the grid voltage feedforward based proportional-integral (PI) controller.The goal of the Smart Grid Initiative (SGI) is to enhance RES grid integration, the deployment of cutting-edge technology, real-time electricity pricing, and metering. One of SGI's primary objectives is the design of power electronics-based SIs [4][5].

In this study, an SPV-based smart inverter (SPV-SSI) is built and analysed. It has the following combined functionalities: managing voltage at the point of common coupling (PCC) during voltage faults or sags; supplying power to local loads; injecting power into the power grid; providing power to utility loads up to the inverter's nominal capacity; storing energy in lead-acid battery banks. The fuzzy PI (F-PI) controller and the fuzzy SMC both address the drawbacks of the conventionally adjusted PI controller. The benefits of a conventional PI and fuzzy logic controller are combined in the F-PI controller (FLC). It has a quicker and better dynamic reaction, is simpler to design, requires fewer parameter updates, and has no steady-state error [6][7]. F-SMC is a nonlinear control method that combines F-PI and SMC into a single controller. Under steady-state conditions, F-PI reduces chattering. SMC reduces the transient state error, providing a quick dynamic reaction and system stability.

1.2 Objectives

The objectives of the work include the following,

1. Creation of a current-control loop for grid-connected operation and a voltage control loop for stand-alone operation.

2. Efficient design of bi-directional DC-DC buck-boost converter (BDC-DCBBC).

3. Designing stable and flexible controllers, such as the FOPI, F-PI controller, and F-SMC, for voltage and current control loops.

4. Comparison of traditionally-tuned PI controllers and developed controllers under various circumstances.

1.3 Organisation of the Report

The complete thesis is organised as follows. It contains six chapters. Chapter 1 includes a brief introduction, the reasons for doing it, and the goals. Chapter 2 discusses the literature review of various control measures. The system's overall design is covered in Chapter 3. Chapter 4 contains the design and implementation of several controllers. Chapter 5 discusses the outcomes of the various controllers' simulations. There is also a comparison of the controllers using the results of the simulation. In chapter 6, the overall conclusion and potential future directions are covered.

Chapter 2

LITERATURE REVIEW

2.1 Introduction

Previous research on single-phase, transformer-free smart inverters for solar systems is included in this chapter.

2.2 Literature Survey

During the power conversion stage, line transformers are widely used in grid-connected photovoltaic (PV) systems. This transformer protects people and avoids leakage currents between the PV system and the earth by maintaining galvanic isolation between the grid and the PV system. Additionally, it ensures that the grid is not subjected to continual current. However, the transformer is large, heavy, and expensive due to its low frequency (50 Hz). Inverter topologies without line transformers are being studied as a replacement for grid-connected PV systems using line transformers [8]. Under these circumstances, the capacitance between the solar array and the earth may result in leakage currents, which would increase electromagnetic emissions.

Ref[9] describe a transformerless, single-phase PV inverter's high-performance and reliable independent control. A DC-DC boost converter was first developed and designed using back-stepping control that is nonlinear. The recommended converter takes out the greatest properly using power point adjusting to changing weather conditions and utilising a reference voltage produced by the Perturb and Observe (PO) algorithm (MPP). Increasing the voltage at

the inverter's input without utilising a transformer in this system is another reason to use the boost converter. This will make the system more affordable and compact. Second, even when there is a substantial load variation at the inverter's output, the single-phase H-bridge inverters was regulated by employing back-stepping control to minimize error between both the inverter's output voltage and the appropriate value.

The single-phase transformerless inverter is commonly used in low-power photovoltaic system which are grid-connected because of its small size, high efficiency, and low price. [10] suggests a brand-new, highly efficient, three-level, single-phase photovoltaic inverter. A 1.2-kW prototype is used to simulate, experimentally validate, and compare the topology to a three-level diode clamped inverter. The results show that the suggested topology maintains the benefits of the three-level diode clamp inverter, such as the absence of changing total common-mode voltage generation, the decreased current ripples, and the high efficiency.

Superjunction MOSFETs are used in [11] a high-reliability single-phase transformerless grid-connected inverter for solar applications to achieve high efficiency. The suggested converter employs two split ac-coupled inductors, and they each run on a separate cycle for the positive and negative half grid cycles. System reliability is improved since the shoot-through problem that typical voltage source inverters experience is eliminated. Dead time is not necessary during the grid zero-crossing and high-frequency pulsewidth modulation switching commutation instants, which boosts the converter's efficiency and the output ac-quality. Superjunction MOSFETs can be used in the proposed inverter without sacrificing reliability or efficiency because the split structure does not present problems with reverse-recovery for the primary power switches.

Many research has focused on grid-connected inverters as a means of efficiently transferring the energy produced by the PV system. These specialisations include, among others, controller design, control strategies, and inverter topologies. The three reference frames—revolving, stationary, and three-phase natural—can be combined to create the present control loop (abc) (dq). A number of controllers are being researched to regulate the steady-state and transient performance of a grid-connected PV system. These controllers include Repetitive Controller (RC), Proportional Resonant (PR), Sliding Mode Controller (SMC), deadbeat controller, hysteresis controller, and Proportional Integral (PI) controller with grid voltage feedforward.

In Reference [12], a cascaded two-level inverter is constructed with an adaptive SMC. In Reference [13], the idea of a neuro-fuzzy DSPAC controller is presented. A grid-based interac-

tive RE system built on fuzzy PI is provided in Reference [14]. In addition, the literature has offered the benefits and drawbacks of various systems in terms of steady-state error and transient responsiveness. The aforementioned controllers improved the grid-connected PV system's performance.

2.3 Conclusion

This chapter examined the features, advantages, and drawbacks of various control strategies utilised in grid-connected renewable energy systems to enhance power quality in light of the available research and practises.

Chapter 3

SYSTEM DESIGN

3.1 Introduction

The system's fundamental architecture is detailed, and each component is described.

3.2 Basic Structure of the System

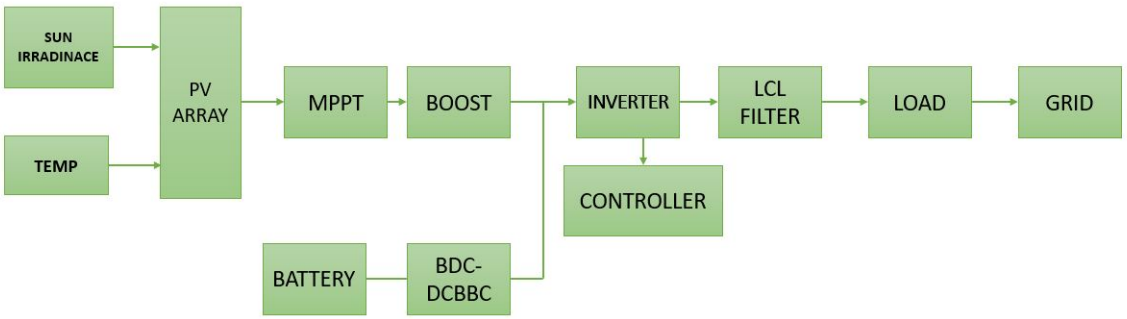

Figure 3.1: Block diagram of the system.

Two converters and an inverter make up the system. where solar or batteries are used to power the grid. For photovoltaics, a boost converter is utilised, and for batteries, a bidirectional DC-DC buck boost converter. The PV system's boost converter is fired under the control of MPPT, which uses the perturb and observe algorithm. A single phase voltage source inverter is utilised in this situation. Smart inverters are essential for managing and integrating distributed energy into the power grid. PI, FOPI, FPI, and FSMC controllers are employed in this case.

3.3 PV Array

Figure 3.2: PV Array

An electric power system that uses photovoltaics to generate usable solar electricity is referred to as a solar power system or photovoltaic system, also referred to as a PV system. It is made up of a combination of several parts, such as solar panels that take in and convert sunlight into power, solar inverters that change the output from direct to alternating current, mounting hardware, wiring, and other electrical components needed to make up a functional system. It might also have an integrated battery and a solar tracking system to enhance the device's overall performance. Contrast PV systems, which directly convert light into energy, with alternative solar heating and cooling technologies like concentrated solar power or solar thermal [15]. The PV system's visible component, the collection of solar panels, is the only component of a solar array; the remaining hardware, which is frequently referred to as the balance of the system, is not included. While massive utility-scale power plants can produce hundreds of megawatts of power, small rooftop-mounted or building-integrated PV systems can only provide a few to few tens of kilowatts. Today, most PV systems are grid-connected, with off-grid or independent systems accounting for a minor portion of the market. Table 3.1 lists the photovoltaic system's specifications.

3.4 Maximum Power Point Tracking

Maximum power point tracking (MPPT) is an algorithm used in photovoltaic (PV) inverters to constantly adjust the impedance seen by the solar array to maintain the PV module's performance at, or relatively close to, the peak power point of the PV panels under a variety of circumstances, such as shifting loads, temperatures, and sun irradiation [16].

Table 3.1: Parameters of PV System

Parameter	Value
Maximum Power, P_{max}	390 W
Irradiance, I_r	$1000W/m^2$
Temperature,T	25°C
Voltage at Maximum Power, V_{max}	40.1 V
Current at Maximum Power, I_{max}	9.73 A
Open Circuit Voltage, V_{OC}	48.85 V
Short Circuit Current, I_{SC}	10 A

The PO approach is frequently used to track the MPP. This method modifies the PV module's power using a small disturbance. Periodically, the PV output power is measured and compared to the preceding power. If the output power increases, the same process is followed; if not, the perturbation is reversed. The PV module or the array voltage is perturbed by this technique. To determine if the power is increasing or decreasing, the PV module voltage is changed. The PV module's operational point is to the left of the MPP when an increase in voltage results in an increase in power. Therefore, to attain MPP, more disturbance is needed to the right [17].

The PV module's operational point is to the side of the MPP, which, on the other hand, demands more disturbance to the left in order to attain the MPP if a rise in voltage results in a loss of power. Fig. 3.3 shows the flowchart of the charge controller's chosen PO algorithm. The PV module and battery voltages are measured by the MPPT charge controller when it is connected between them. After determining the battery voltage, it determines if the battery is fully charged or not. To avoid battery overcharging, charging stops once the battery reaches full charge.

The PO MPPT algorithm operates as follows, which summarises its functionality:

1. Power is increased; if the previous state's perturbation was positive, the power rise is continued in that direction.

2. The power is reduced when the previous state was negatively perturbed, and the current perturbation should be in the opposite direction.

3. If the perturbation of the state before it was negative, the power is raised and the perturbation is then carried out in the same direction.

4. If the previous state had undergone a negative perturbation, the current perturbation should travel in the opposite direction.

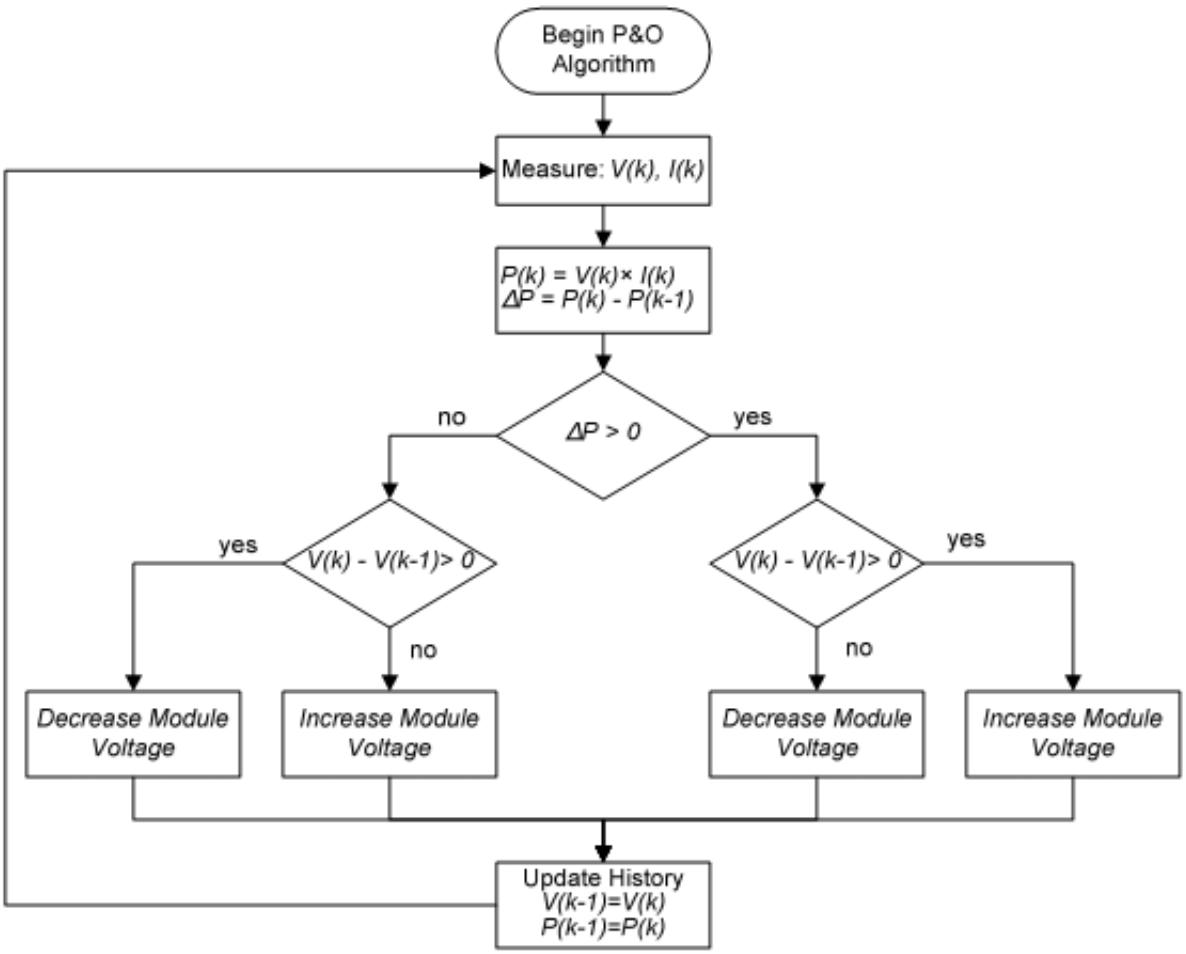

Figure 3.3: P and O MPPT Algorithm.

3.5 Battery

A lithium-ion battery, sometimes known as a "Li-ion battery," is a category of rechargeable battery made up of cells in which, during discharge, lithium ions travel from the negative electrode to the positive electrode through an electrolyte, and vice versa, during charging. A

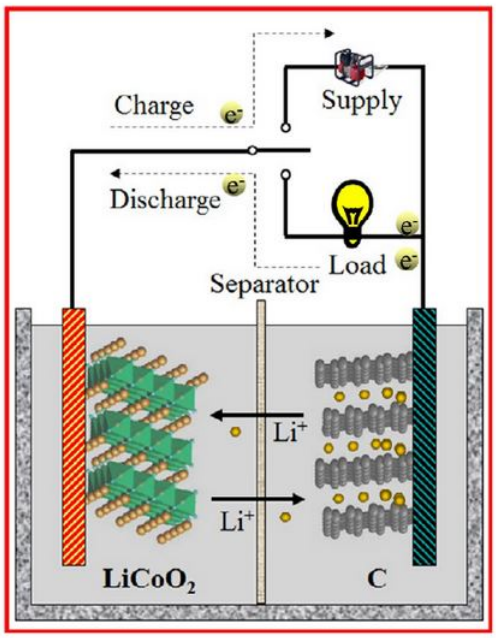

Figure 3.4: Li-ion Battery

lithium intercalated substance serves as the lithium-ion battery positive electrode, while graphite is typically used as the negative electrode. Compared to LFP cells, lithium-ion batteries have a greater energy density, no storage effect, and a lower self-discharge rate. Energy or power density can be given preference while making cells. However, they can be hazardous due to the flammable electrolytes they contain, which, if broken or charged incorrectly, can result in flames and explosions [18].

Two important essential characteristics that Li-ion batteries may display are a longer cycle life and a reduced life cycle cost. When lifespans are taken into account, Li-ion batteries may have lower cost per cycle than lead-acid batteries. Therefore, even with the current state of development, it would be better to invest in Li-ion rather than lead-acid even though the initial cost is higher. The distinctive energy storage offered by renewable energies, however, is not deemed enticing enough by Li-ion industrials for large-scale manufacture.

Basic Li-ion cells are joined together in parallel or series to enhance voltage or in combination to boost current in a Li-ion battery. A module can incorporate several battery cells. A battery pack can integrate many modules. In a typical Li-ion cell, the cathode (positive electrode) and anode (negative electrode) are in contact with an electrolyte that contains lithium ions. Typically, depleted materials are used to build commercial cells. LiCoO2, LiFePO4, and carbon are employed as anodes in discharged cathodes because they are stable in the atmosphere

Table 3.2: Battery parameters

Parameter	Value
Nominal Voltage	190 V
Rated Capacity	24 Ah
Initial SOC	80 %
battery Response Time	1 sec

and easy to handle in industrial processes. The two electrodes are linked to an external electric system externally during the charging process. The electrons are forced to leave the cathode and travel to the anode's surface. Internally, concurrently, the lithium ions move through the electrolyte from the cathode to the anode. In this manner, the external energy is electrochemically stored in the battery as chemical energy in the materials of the anode and cathode, which have various chemical potentials. During the discharging process, the opposite happens: Li ions migrate from the anode to the cathode in the electrolyte while electrons flow from the anode to the cathode through the external load to perform the work. During charge and discharge cycles, Li ions alternate between the anode and the cathodes, giving rise to the mechanism's nick-name, "shuttle chair".

3.6 Boost Converter

One of the most basic types of switch-mode converters is the boost converter, often known as the step-up converter. As its name suggests, the converter raises an input voltage. In other words, it serves the same purpose as a step-up transformers by maintaining the same amount of power output while increasing the Voltage level from low to higher and decreasing the flow from high to low [19].

A capacitor, a diode, an inductor, and a semiconductor switch are its only components. Because they were initially created and developed in the 1960s to power electronics on aircraft, boost converters are fairly straightforward and only need a small number of components. A boost converter's highest benefit is its extremely high efficiency. The fundamental idea underlying the boost converter is the inductor's propensity to resist changes in current by either

storing more or less energy in its magnetic field. A boost converter's output voltage is always higher than its input voltage.

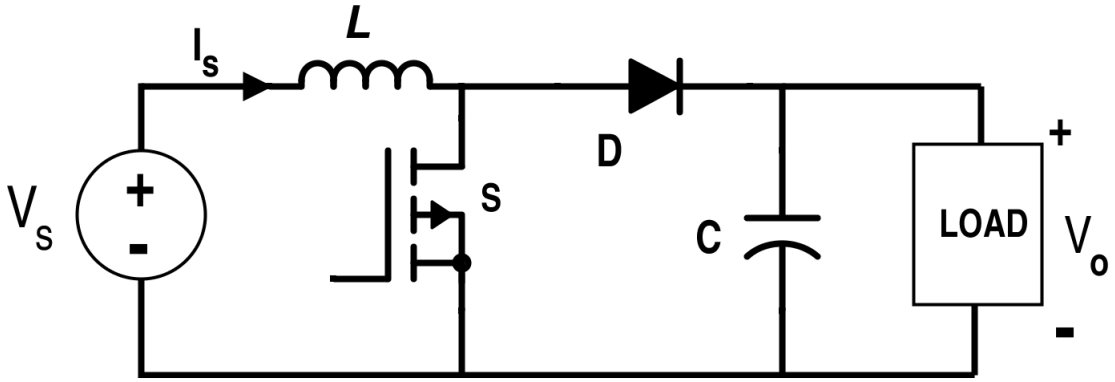

Figure 3.5: Boost Converter

Figure 3.6 shows a basic boost converter. The inductor generates a magnetic field and current flows through it clockwise when the switch is closed (in the "on" state), allowing the inductor to store some energy. The inductor's left side has positive polarity. As a result of the larger impedance in the open (or "off-state") state of the switch, current will be reduced. In order to maintain the current flowing in the direction of the load, the magnetic field's previously created energy will be lowered. The result is a change in polarity.

Due to the series connection of the two sources, a larger voltage will be used to charge the capacitor through the diode D. Between charging stages, the inductor won't completely drain if the switching is cycled quickly enough, and the load will always experience a voltage when the switch is opened that is greater than the of the input source alone. While the switch is open, this total voltage is also applied to the capacitor connected in series with the load. The capacitor can thus supply the load with voltage and energy when the switch is then closed, shorting the right side from the left side. The blocking diode stops the capacitor from discharging during this time through the switch. Obviously, the switch needs to be opened rapidly enough to prevent excessive capacitor discharge. The current flowing through the inductor never reaches zero when a boost converter is in continuous operation. The DC (average) voltage across an inductor must be zero in the steady state for the inductor to return to its initial condition after each cycle since the voltage across an inductor is inversely proportional to the rate of change of the current

flowing through it. The ideal transfer function is given as:

$$V_o/V_i = 1/(1-D) \tag{3.1}$$

3.7 Bi-directional DC-DC Converter

In contrast to a typical buck-boost converter, which can only control energy flow in one way, a bidirectional converter can control power flow in both directions. In order to step-up or step-down voltage levels and move power either forward or backward, bidirectional dc-dc converters are required. Bidirectional dc to dc converters have the ability to manage the flow of power between two dc sources and a load in both directions by using a special switching approach and phase-shifted control strategy. As a result, any surplus energy produced can be kept in batteries or another type of storage.

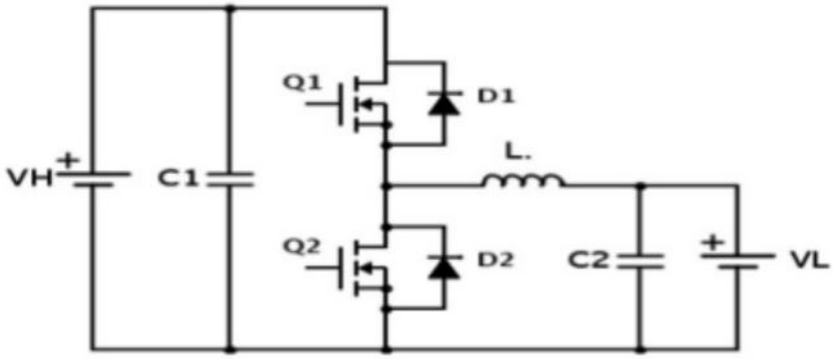

Figure 3.6: Bi-directional DC-DC Converter

The aforementioned circuit can operate in either buck or boost mode depending on how the Mosfets Q1 and Q2 are turned. Depending on how the Mosfets Q1 and Q2 are swapped, the circuit can run in either a buck or a boost mode. In response to the switches Q1 or Q2, With a diode that spins freely, the circuit either increases or decreases the voltage connected across the anti-parallel diodes D1 or D2, as appropriate. The two modes listed below are how the aforementioned circuit operates in both directions:

1. Switch Q2 and diode D1 conduct in mode 1 (Boost Mode), whereas switch Q1 and diode D2 are always off. This is because of the duty cycle. Additionally, based on the conductivity of the switch Q1 and this mode can be split into two intervals using the diode D2.

2. Since Q2 is on in this mode and may therefore be investigated to be short-circuited, the inductor current rises during interval 1 (Q2-on, D2-off; Q1-off, D2-Off). This is because the lower voltage battery charges the inductor during this time period. Additionally, since the switch Q1 is off and the diode D1 is reverse biassed in this mode, no current enters the switch Q1.

3. Interval 2 : In this mode, Q2 and Q1 are both off, making them open circuits. The voltage crossing the resistor has now changed polarity since the current flowing into the inductor, which is operating in circuits with the voltage source, cannot be changed instantly. As a result of the diode D1 being forward biassed, the output capacitor C2 is charged to a higher voltage by the inductor current. As a result, the output voltage increases.

4. In mode 2, switch Q2 and diode D1 are always off, but switch Q1 and diode D2 begin to conduct when the duty cycle is reached. Additionally, based on the conductivity of the switch Q2 and the diode D1, this mode can be divided into two intervals.

5. Interval 1: Q2 is off while Q1 is on. Both the lower voltage battery and the large voltage batteries will recharge the inductor and o/p capacitor, respectively.

6. Interval 2: In this mode, Q2 and Q1 are both off. The inductor current is discharged via the freewheeling diode D2 once more because it cannot vary instantly. According to how the input voltage is associated, the voltage across the load is reduced.

The nominal inductor current I_L for the buck-boost is calculated as:

$$I_L = \frac{P}{V_B} \tag{3.2}$$

The inductor's value is created by Equation(3.2). L restricts the ripple current on the DC link to 50% of I_L.

$$L = \frac{V_B \left(V_{dc} - V_B\right)}{f_6 V_{dc} \times 0.5 \times I_{Ji}} \tag{3.3}$$

$$C_1 = \frac{0.5 I_L}{8 f_s \times 0.001 \times V_B} \tag{3.4}$$

The boost capacitor C_2 is constructed similarly Equation(3.5). The ripple voltage in the DC link is restricted to 0.1% of V_{dc}.

$$C_2 = \frac{P \left(V_{dc} - V_B\right)}{f_s \times 0.001 \times V_{dc}^3} \tag{3.5}$$

3.8 Single Phase Inverter dq Implementation

The control is created with the use of a revolving reference frame. From single-phase quantities, two orthogonal components with a virtual q-axis are produced. The real component is either delayed by 1/4 of its own time or the fundamental signal is derived to produce the virtual component. The derivative approach is introduced in [20]. The following is a presentation of the inverter's needed output signal:

$$x_\alpha(t) = A_\alpha \cos(\omega t + \phi) \tag{3.6}$$

where $x_\alpha(t)$ is the inverter's needed output signal, A_α is the signal's amplitude, ω is the output voltage's fundamental frequency, and ϕ is the original system's phase angle [21].

$$x_\beta = \frac{\mathrm{d}}{\mathrm{d}x} x_\alpha(t) \tag{3.7}$$

where x_β is the variable and x is the first derivative of the output equation (current or voltage).

$$x_\beta = A_\beta \sin(\omega t + \phi) \tag{3.8}$$

where A_β is the fictitious system's amplitude. After calculating the derivative of $x_\alpha(t)$, A_β becomes:

$$A_\beta = -\omega A_\alpha \tag{3.9}$$

The imaginary component is obtained by delaying the real component by 1/4 of its own period. Figure 3.7 depicts a single-phase PLL structure with a T/4 delay, where V_α,V_β,V_d,V_q are the voltages of the different axes, and 0 is the output voltage's starting fundamental frequency. It is applied to the dq transformation as follows:

$$\begin{bmatrix} X_d \\ X_q \end{bmatrix} = \begin{bmatrix} \cos(\omega t) & \sin(\omega t) \\ -\sin(\omega t) & \cos(\omega t) \end{bmatrix} \begin{bmatrix} x_a \\ x_\beta \end{bmatrix} \tag{3.10}$$

3.9 Voltage and Current Control Loops

The inverter runs on a voltage control loop and a current control loop. A stand-alone inverter has a voltage control loop, whereas a grid-connected inverter has a current control loop. In this section, the inverter's thorough description is covered. It exclusively address control

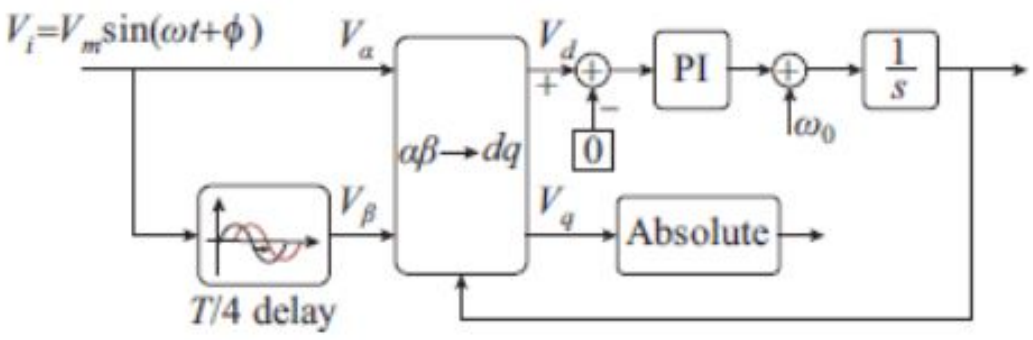

Figure 3.7: T/4 delay based single phase PLL structure

loop implementation in this study. PLL provides the phase angle and frequency information. PI controllers produce the SPWM (sinusoidal pulse width modulation) modulator references.

$$A_{ref} = \sqrt{D^2 + Q^2} \tag{3.11}$$

$$\phi_{ref} = \alpha \tan(g) \frac{Q}{D} \tag{3.12}$$

where D and Q are the corresponding values of the d- and q-axes, respectively, and A_{ref} is the sinusoidal amplitude, ϕ_{ref} is the phase angle reference. As a reference voltage, V_{dref} is set to 1 and V_{qref} to 0. The active and reactive reference power, or P_{ref} and Q_{ref}, are used to determine the current references I_{dref} and I_{qref}. The output line currents that have already been converted to dq reference frame are contrasted with the computed currents. The inaccuracy is reduced by using a PI controller to produce the necessary sinusoidal reference for an SPWM modulator.

$$A = \frac{\sqrt{P_{PU}^2 + Q_{PU}^2}}{V_{2PU}} \tag{3.13}$$

$$\phi_{I_\phi} = \alpha \tan(g) \frac{Q_{PU}}{P_{PU}} \tag{3.14}$$

$$I_{ref}r(t) = A_{I_M} \sin\left(\omega t + \phi_{I_{ref}}\right) \tag{3.15}$$

where P_{PU} and Q_{PU} are the active and reactive components of the power, respectively; A_{Iref} is the reference current's amplitude; I_{ref} is the sinusoidal value of the reference current and V_{2PU} is the local load voltage. The angle t is acquired at the LCL filter output from the PLL of voltage V_{2PU}.

3.10 Conclusion

This chapter described the overall architecture of the system. Each system component's design and a brief description are also supplied. In the following chapter, controller design is covered.

Chapter 4

CONTROLLER DESIGN

4.1 Introduction

This chapter compares and explains controllers. There are several types of controllers: fuzzy proportional integral, fuzzy sliding mode controller, and fractional order proportional integral.

4.2 Proportional Integral

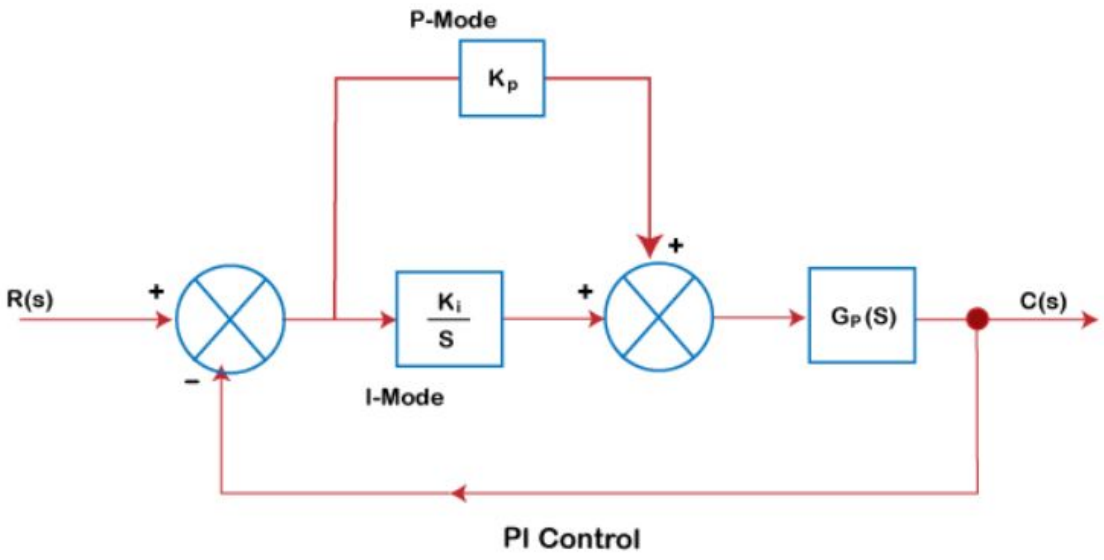

Figure 4.1: Basic Structure of Proportional Integral Controller

Integral control is employed when we want the controller action to return the desired reference signal from any constant and ongoing offset. Processes with slow to moderate speeds typically employ the proportional integral controller. We are aware that an integral controller tends to make the system less stable overall. By including a proportional controller, it can be overcome. The Integral controller's block diagram is displayed below. As a result, the proportional mode is usually used in conjunction with the integral controller to give the automatic next action that eliminates the proportional offset. The PI controller's output is the union of their individual gain constants, as can be seen in the example below:

$$\mathbf{V}_0 = \mathbf{K_p e} + \mathbf{K_i} \int \mathbf{e dt} \tag{4.1}$$

When the proportional mode is unable to minimise the offset to the appropriate level on processes with a significant load variation, the PI controller is also utilised. The reset action offered by the Integral controller eliminates the proportional offset.

4.3 Fractional Order Proportional Integral

The integro-differential processes of fractional orders are a part of the advanced fractional calculus, a development of conventional integer-order calculus. Fractional-order calculus has gained a lot of attention recently because it is the best representation of many processes in physics, chemistry, and engineering that exhibit a memory effect [22].The accurate and quantitative solutions of the fractional-order integro-differential equation have drawn a lot of attention because system applications have advanced. Fractional-order systems can have their behaviour modified using integer or fractional-order control approaches. It has been demonstrated that controllers with fractional orders frequently perform better than their counterparts with integer orders [23].

The most of physical processes are by their very nature fractional ordered. As a result, it is more accurate to adjust the dynamic response of a control system that used a fractional order controller as opposed to a traditional PI controller. The cost incurred is the challenging tuning of the fractional order system as a result of the additional parameter [24]. The improved precision predicted by using the fractional order calculus was not achieved up until this point because it was approximately similar to integer calculus. The fractional order calculus can be changed in a variety of ways nowadays.

The FOPI is defined using the Riemann-Liouville definition for continuous models and the Grunwald-Letnikov definition for discrete models.

$$U(t) = K_p e(t) + K_i D^{-\lambda} e(t) \tag{4.2}$$

This show how the FOPI is defined by Grunwald and Letnikov. Figure depicts the block diagram of the suggested FOPI controller.

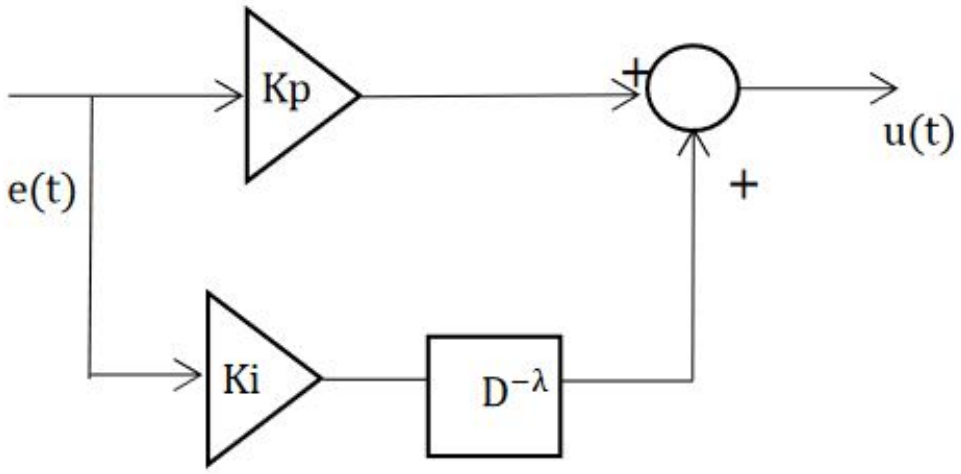

Figure 4.2: Structure of FOPI controller

4.4 Fuzzy Logic Controllers

Fuzzy logic uses verbal equations rather than intricate mathematical formulas to express the operational laws. The use of conventional control methods is typically not feasible since it is challenging to accurately simulate many systems with these complex equations. The operational properties of such systems can be defined, however, using the language words of fuzzy-logic [25]. The fundamental benefit of fuzzy logic is that it doesn't need a complicated mathematical model, therefore it can process rules using very straightforward mathematical operations. Additionally, it has been demonstrated that the operations in fuzzy-logic approaches utilising max-min composition correspond identically to the rapid universal computation scheme [26].An expert-based set of linguistic description rules are employed in a fuzzy-logic controller to explain a fuzzy system's dynamic behaviour [27]. The following are typical formats for the specialised knowledge: If input 1 is large and/or input 2 is small, then (output 1 is negative large and (output 2 is positive small)) $\cdots$ (inputN is medium) (outputM is zero).

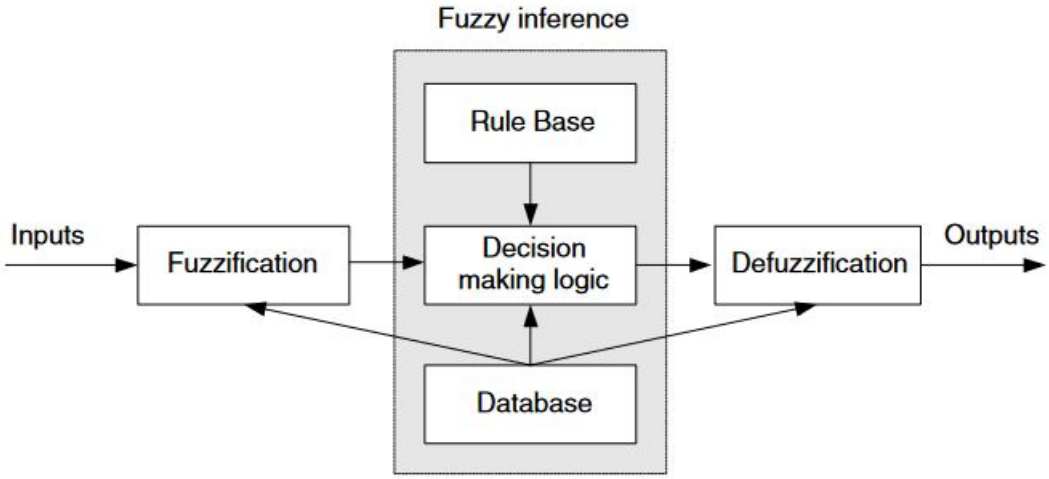

Figure 4.3: Fuzzy Logic Controller

In essence, fuzzy-control rules offer a practical means of communicating domain knowledge and control policy. Furthermore, both the antecedents (before then) and the conclusions (after then) of these rules may involve a number of linguistic variables. Symbolic controllers can be thought of as a specific class that includes fuzzy-logic controllers. Fig. 1 depicts the configuration of the fuzzy-logic controller block diagram. The three characteristics of symbolic controllers are fuzzy inference, defuzzification, and fuzzy inference. The real variables are transformed into linguistic variables throughout the fuzzification process using fuzzy-set theory. The "if-then" rules that specify the behaviour of the system are assessed during the fuzzy-inference step. Using the specified rule basis, the defuzzification stage converts the linguistic outcome of the fuzzy inference back into a real value.

Fuzzification, rule-base, inference mechanism, and de-fuzzification make up FLC's four key structural components.

1. Fuzzification: This is also known as the fuzzifier. Using fuzzy linguistic variables, linguistic terms, and membership functions, the system's real or crisp data are mapped into a fuzzy set during the input interface process.

2. Rule Base: A group of IF-THEN rules with an ambiguous condition and conclusion is known as a "rule base." These rules define the action to be taken by the controller by controlling the output variable in terms of the input variables.

3. Inference Mechanism: A fuzzy inference engine or inference engine are other names for this procedure. This stage involves evaluating and using the expert's knowledge of the

regulations in order to establish the best strategy to control the plant. In essence, it entails reexamining and deleting regulations.

4. De-fuzzification: This process is also known as the de-fuzzifier. The output mapping interface provides the controller work for the plant by converting the fuzzily inputted data from the inference engine into crisp, real-time output.

4.4.1 Fuzzy PI

The proportional kp and ki integral, which make up the PI controller's parameters, remain constant. The performance of the PI controllers declines and tunes when the system experiences sudden disturbances or parameter uncertainty. As a result, an adaptive PI controller that modifies its parameters in accordance with the error function is needed [28]. Fuzzy rules are used in this controller's PI controller, which is shown in Table 4.1 and listed as:

1. If the error absolute $|e(t)|$ is zero, then k_p is large and k_i is small.
2. If the error absolute $|e(t)|$ is small, then k_p is large and k_i is zero.
3. If the error absolute $|e(t)|$ is large, then k_p is large and k_i is large.

FRs are straightforward if-then statements that produce conclusions based on conditions. Triangular membership function (TMF) is the membership function used in fuzzification and defuzzification phases to transfer crisp/real input into fuzzy output and vice versa. TMF is specified as:

$$\mu_A(x) = \begin{cases} 0 & x \leq a, x \geq b \\ \frac{x-a}{m-a} & a < x \leq m \\ \frac{b-x}{b-m} & m < x < b \end{cases} \tag{4.3}$$

where m is the peak value of TMF and a, b, and are the lower and upper limits, respectively. Additionally, amb The output of a straightforward PI controller is denoted mathematically as:

$$\frac{V_{dq}}{I_{dq}} = K_p e(t) + K_i \int e(t)\mathrm{d}t \tag{4.4}$$

The output of the voltage controller for islanded mode is V_{dq}, while the output of the current controller for grid-connected mode is I_{dq} in the equation above.

Table 4.1: IF-THEN rules for Fuzzy-PI and F-SMC

Input Membership Function			**Output Membership Function**		**IF-THEN Rules**	
S.No.	Linguistic Terms	Range	Linguistic Terms	Range	IF Input $\|e(t)\|$	THEN output (k_p,k_i)
1	Zero	[0,0.2]	Zero	[0,0.2]	Zero	Zero
2	Small	[0.3,0.7]	Small	[0.3,0.7]	Small	Small
3	Large	[0.8,1.0]	Large	[0.8,1.0]	Large	Large

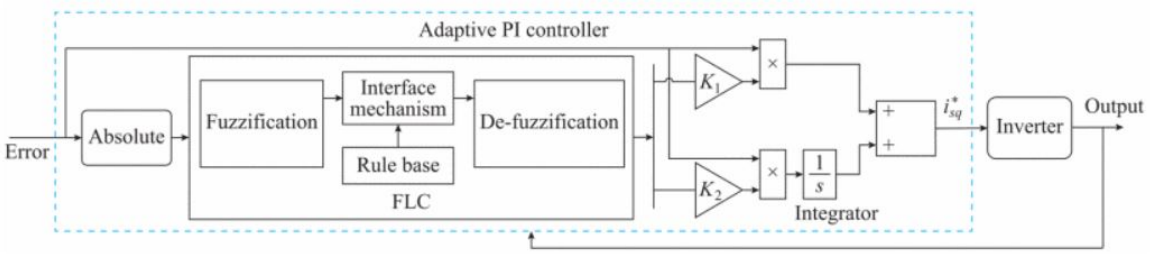

Figure 4.4: Structure of F-PI Controller

The PI gains of the F-PI controller are updated using FR in order to reduce mistakes. The output equation for the created fuzzy controller is shown in equation.

$$\frac{V_{dq}}{I_{dq}} = F_1 K_1 e(t) + F_2 K_2 \int e(t)\mathrm{d}t \tag{4.5}$$

where F_1 and F_2 are the outputs of the fuzzy controller for Kp and Ki, respectively, and K_1 and K_2 are the learning rate gains for Kp and Ki, respectively.

4.4.2 FSMC

A well-known, reliable control method known as the sliding mode controller (SMC) may guarantee excellent tracking even when the system is subject to both internal and external disturbances. In addition to these other characteristics, SMC is characterised by its high precision and simplicity. The designing of a sliding mode controller for a dual PMSM is the subject of this chapter. In the face of inaccurate modelling, the sliding mode controller is a nonlinear control approach for preserving performance stability and consistency. Two modes make up the majority of the SMC. The first phase is the reaching phase, and the second is the sliding phase, as shown in Fig. 4.6.

According to a rule that is based on the value of the state at any given moment, the gains of each feedback path alternate between two values. The purpose of the switching control rule is to steer the state trajectory of the nonlinear plant onto a specified (user-selected) surface in the state space and hold it there for a subsequent amount of time. It is referred to as a switching surface. A feedback path has one benefit if the plant state trajectory rises "above" the surface and a separate gain if it lowers "below." This surface defines the appropriate switching protocol.

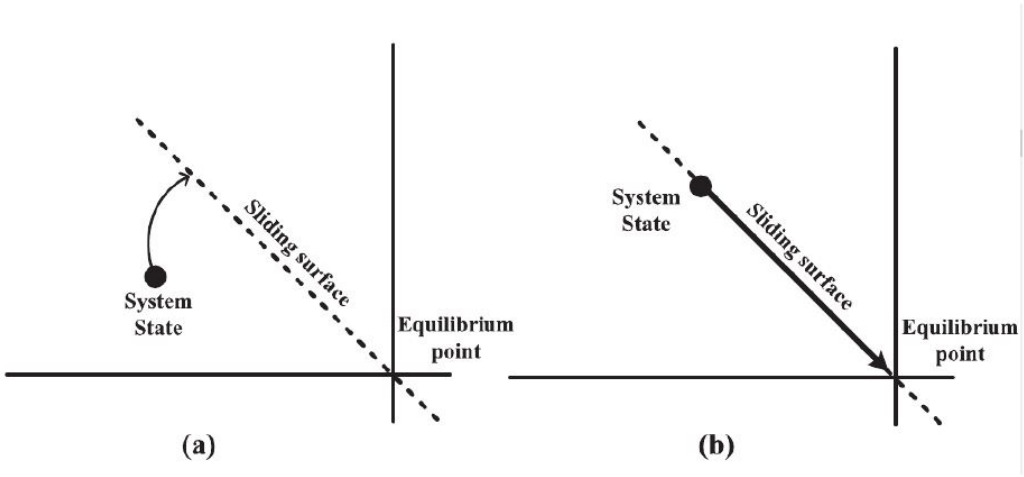

Figure 4.5: Reaching and sliding phase

Alternatively known as a sliding manifold, this region is called a sliding surface. In a perfect world, the switched control preserves the plant's state trajectory on the surface for the duration of the following period and the trajectory slides across the surface after being intercepted. The hardest problem is creating a switched control that will send the plant state to the switching surface and keep it there when it is intercepted. The Lyapunov method is used to explain this problem.

There are only two steps in the controller design technique. The sliding condition is first confirmed using a feedback control law. To accommodate for modelling uncertainty and disturbances, the control rule must be discontinuous over the sliding surface. Chattering results from an incorrect implementation of the associated control switching and is undesirable in practise because it demands high control activity and could trigger high-frequency dynamics that were disregarded during modelling. Because of this, the discontinuous control law is sufficiently smoothed in a subsequent phase to offer the optimal control bandwidth and tracking accuracy trade-off. Robustness against parametric uncertainty is acquired in the first step, while robustness against unmodeled high-frequency dynamics is attained in the second.

Chattering is minimised by minimising the control discontinuities in a thin boundary layer near the switching surface. A fuzzy logic control technique and the Sliding Mode Control algorithm are combined in the Fuzzy Sliding Mode Controller (FSMC) (SMC). It is generally known that the sliding mode control algorithm can offer resilient system performance and strong transient performance. However, these performances have a few drawbacks: the system is continually under high control to ensure its convergence to the target state, which is undesired; the chattering phenomena that develop due to the discontinuous part of the control, which might harm the motors [29]. A fuzzy controller must be utilised in conjunction with the sliding mode control to achieve a reliable and fluid control.

In F-SMC, the planned controller is updated using both the F-PI controller and the SMC, two adaptive nonlinear techniques. The F-SMC combines the best aspects of the SMC and F-PI controller. SMC minimises the transient-state error. As a result, the system stability is improved and a quick dynamic reaction is guaranteed. In steady condition, Fig. 4.6 displays the chattering that the F-PI controller and F-SMC reduced.

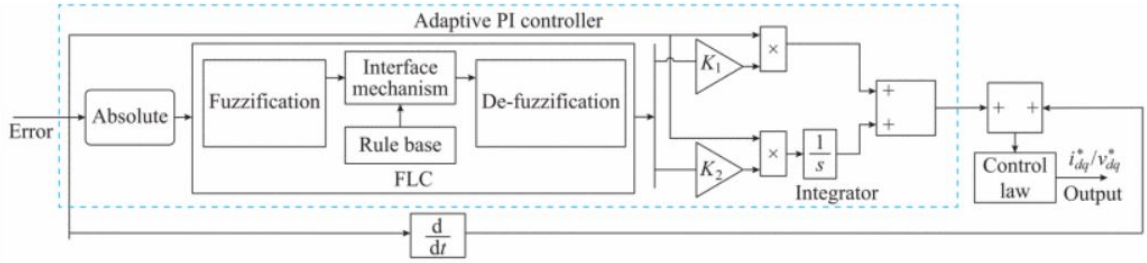

Figure 4.6: Structure of F-SMC Controller

Update gains Kp and Ki for sliding surfaces using FRs (SS). Additionally, SS is created with F-PI controller control law updates. A continuous smooth approximation serves as the foundation for the control law. The SMC mistake and its derivative are always focused on SSe. SS S(t) is defined by the error and its derivative as:

$$S(t) = \dot{e}(t) + \lambda e(t) \tag{4.6}$$

where λ is a random constant and the bandwidth dependant. Additionally, e(t) is defined as:

$$\lambda e(t) = F_1 K_1 e(t) + F_2 K_2 \int e(t)\mathrm{d}t \tag{4.7}$$

The F-PI controller is used to update the value of e. Based on a discontinuous function, the following is the SS control law:

$$\frac{V_{dq}}{I_{dq}} = -U\,\mathrm{sgn}(S) \tag{4.8}$$

where sgn(S)=U when S>0 and sgn(S)=U when S0; U is the bulky positive constant. The electrical system uses PWM control signals, and the oscillation is caused by the discontinuous control law. An alternative is to construct a continuous smooth estimation-based control law that reduces the chattering phenomenon.

$$\frac{V_{dq}}{I_{dq}} = -U\,\mathrm{sat}(\sigma;\varepsilon) = \left[-U\frac{S}{|S|+\varepsilon}\right] \varepsilon > 0, \varepsilon \approx 0 \tag{4.9}$$

where $U\,\mathrm{sat}(\sigma;\varepsilon) = U$ when $(\sigma;\varepsilon)$ >0 and $U\,\mathrm{sat}(\sigma;\varepsilon) = -U$ when $(\sigma;\varepsilon)$ <0.

4.5 Conclusion

This chapter covered the general design of various controllers, including PI, FOPI, FPI, and FSMC. The outcomes of the simulation are shown in the chapter that follows.

Chapter 5

SIMULATION RESULTS

5.1 Introduction

This chapter compares and contrasts traditionally tuned pi controllers with developed controllers under various scenarios.

5.2 Open Loop Simulation Result

It takes highly dependable and adaptable control to effectively connect scattered generation to the grid. Because of this, it is difficult to make real-time decisions without a controller because voltage is not controlled during voltage sags or failures.

A control mechanism ought to be necessary to power loads, add electricity to the grid, power utility loads up to the inverter's nominal capacity, modify voltage during outages, and make judgments based on current prices. To address the deficiencies, FOPI, FPI, and FSMC were developed.

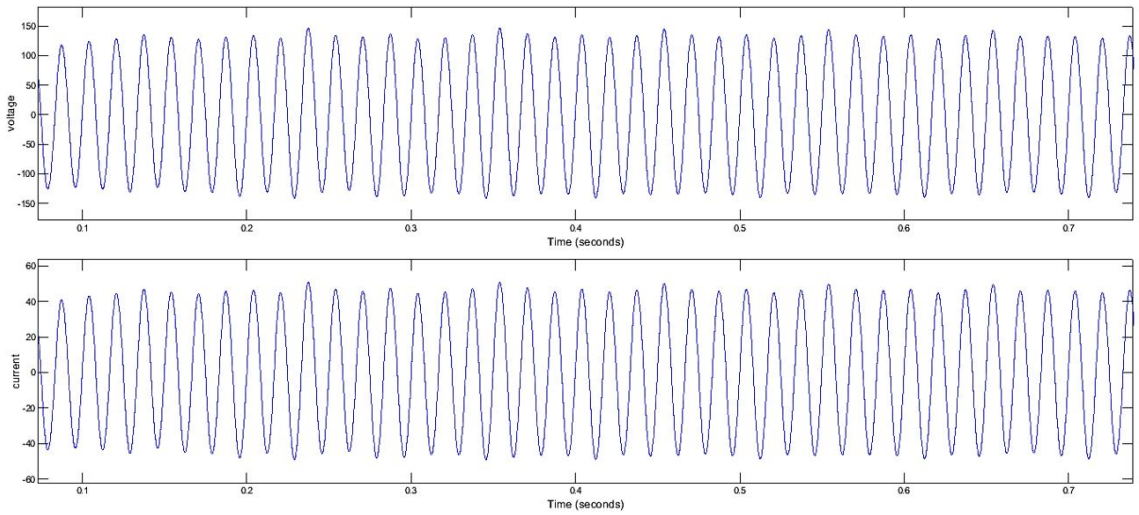

Figure 5.1: Standalone without controller

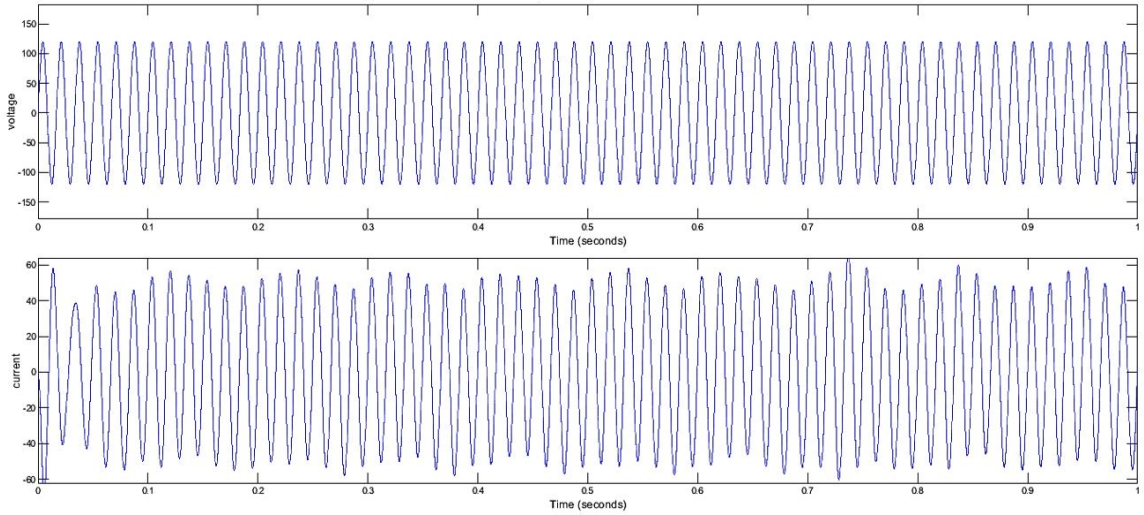

Figure 5.2: Grid connected without controller

5.3 PI - Simulink Results

The effectiveness of a typically tuned PI controller is demonstrated here. Here, the output is not entirely under control. The standalone mode has an overshoot of 1.85% and a 0.15sec settling time. The grid connected mode provides an overshoot of 2.15% and a settling point of 0.15 seconds.

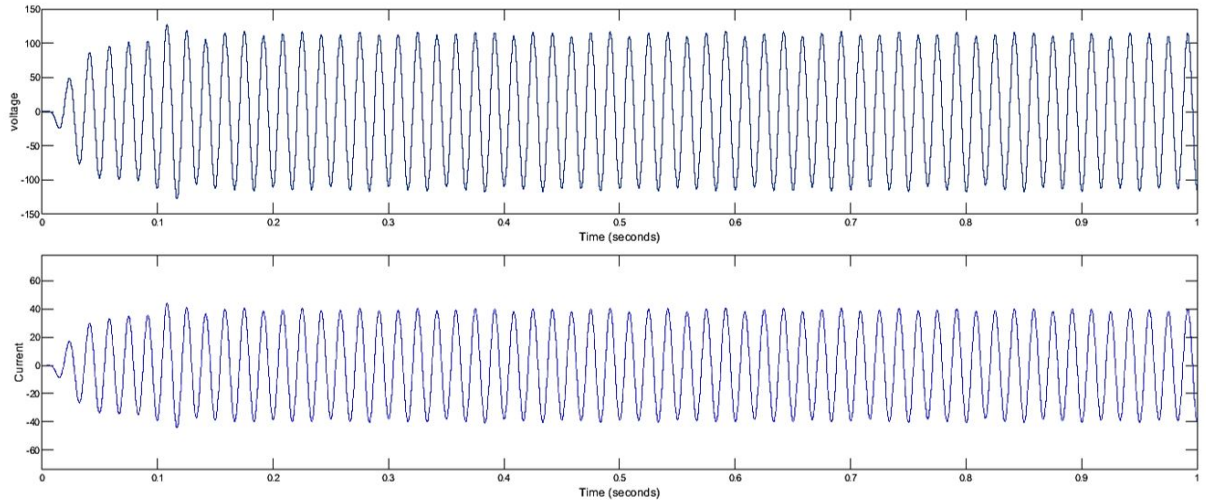

Figure 5.3: PI controlled standalone mode

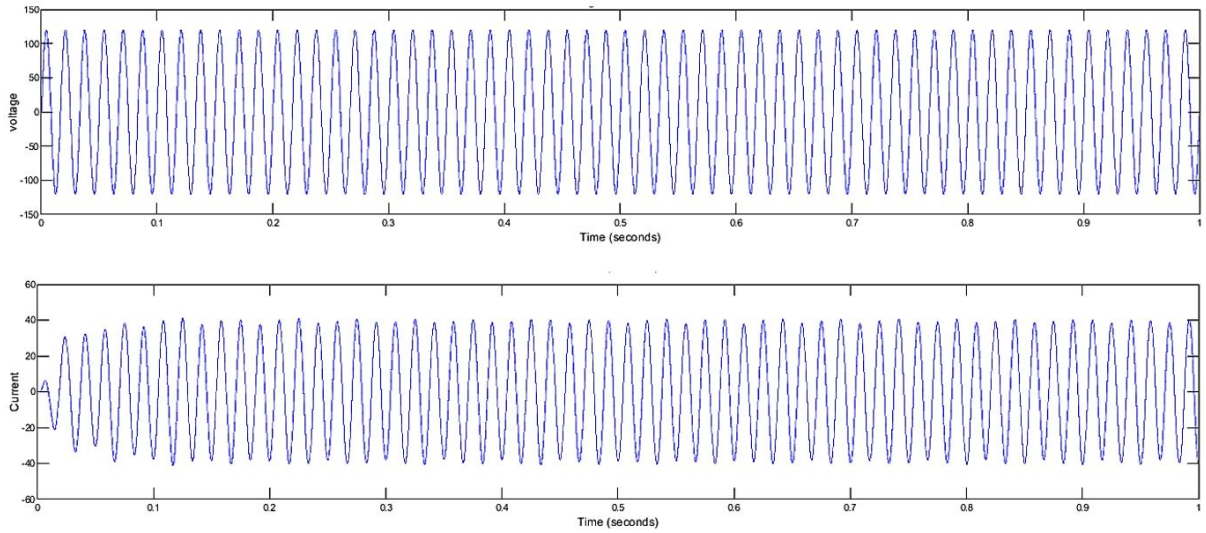

Figure 5.4: PI controlled grid connected mode

5.4 FOPI - Simulink Results

Here the voltage and current is controlled by Factional order proportional integral controller. Standalone mode features settling time of 0.125sec and overshoot of 1.8% and grid connected mode of settling time 0.125sec and overshoot of 2.1%.

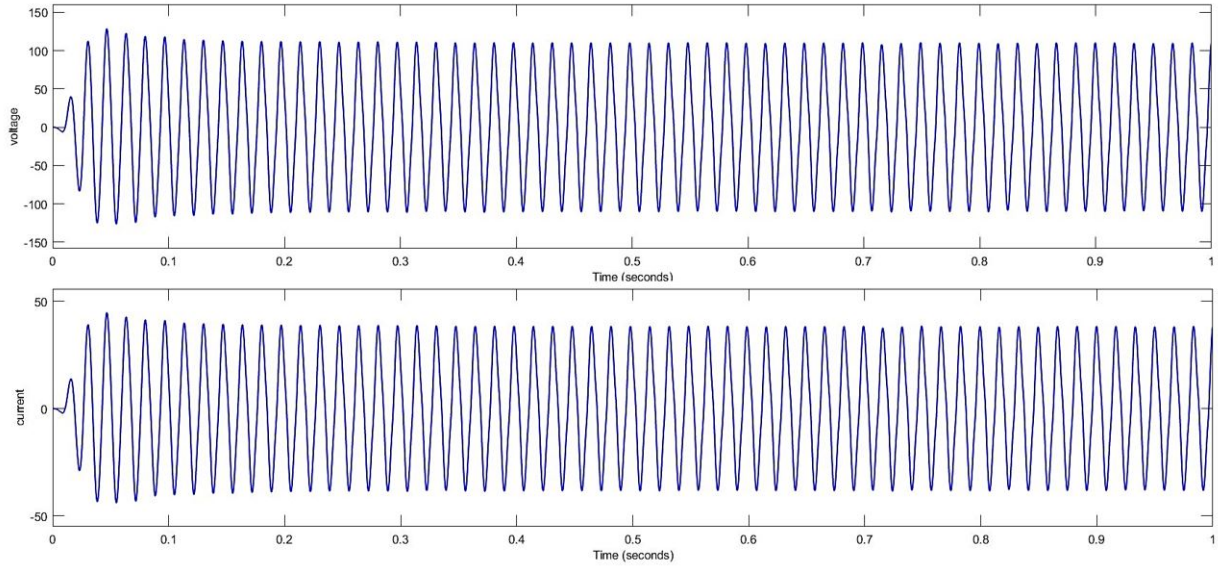

Figure 5.5: FOPI controlled standalone mode

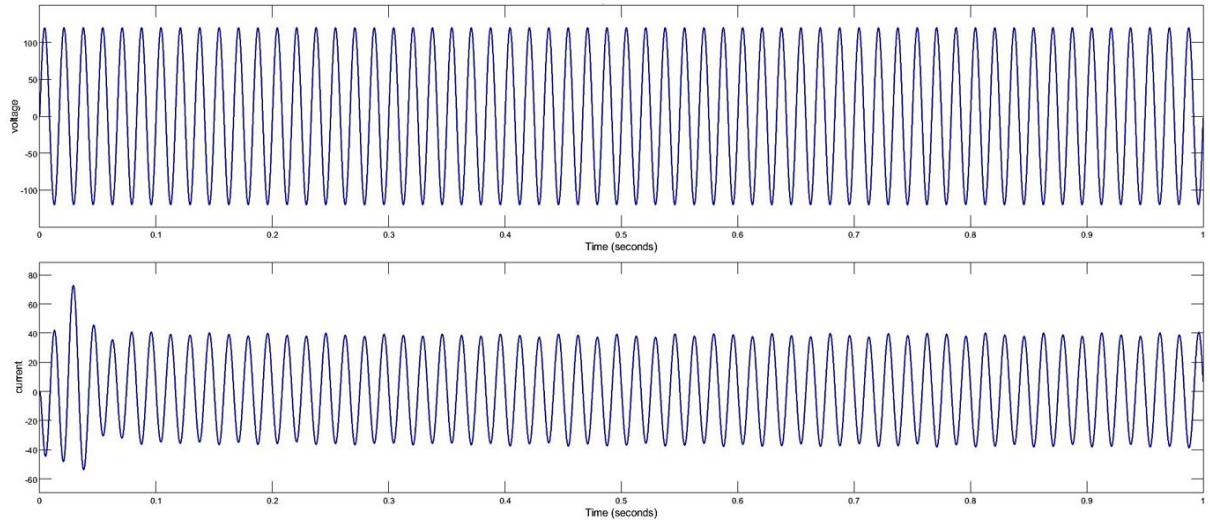

Figure 5.6: FOPI controlled grid connected mode

5.5 Fuzzy PI - Simulink Results

In this scenario, a Fuzzy proportional integral voltage and current are managed by a controller. Grid linked mode has a settling time of 0.1sec and an overshoot of 1.98%, while standalone mode has a 0.08sec settling time and 1.75% overshoot.

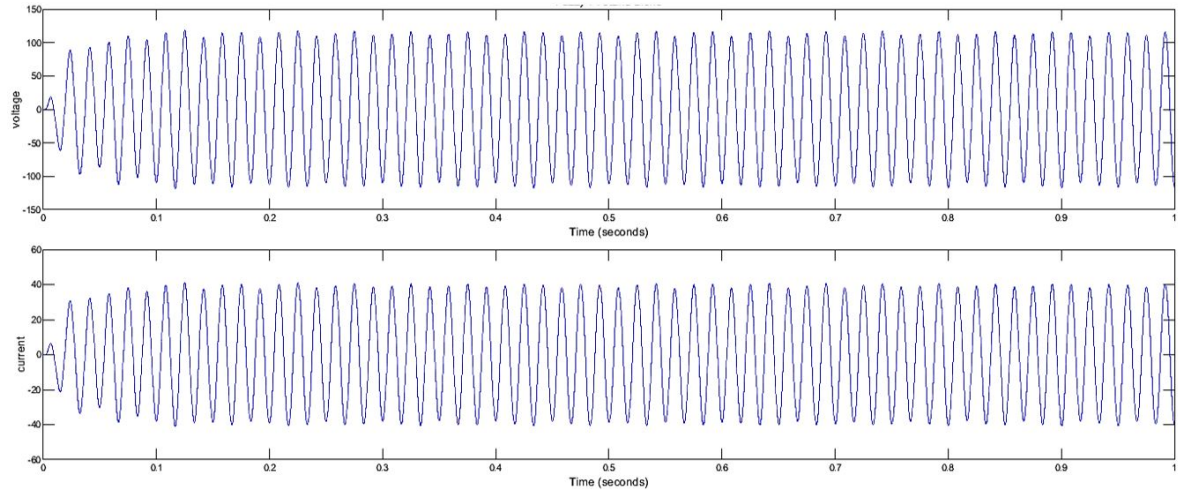

Figure 5.7: Fuzzy PI controlled standalone mode

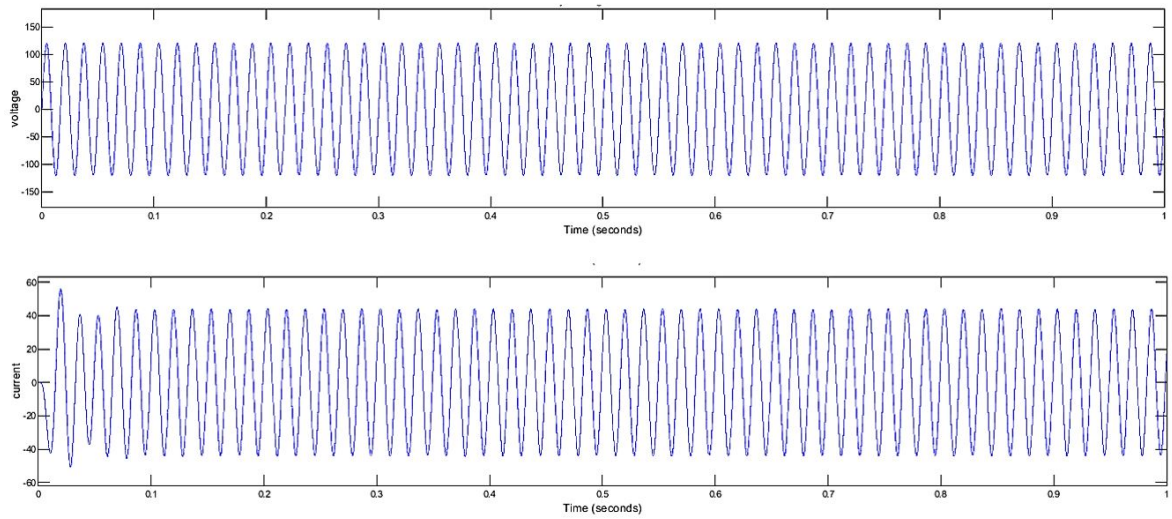

Figure 5.8: Fuzzy PI controlled grid connected mode

5.6 Fuzzy SMC - Simulink Results

Here, a Fuzzy sliding mode controller is used to manage the voltage and current. Grid linked mode has a settling time of 0.08sec and an overshoot of 1.8%, while standalone mode has a 0.075sec settling time and 1.7% overshoot.

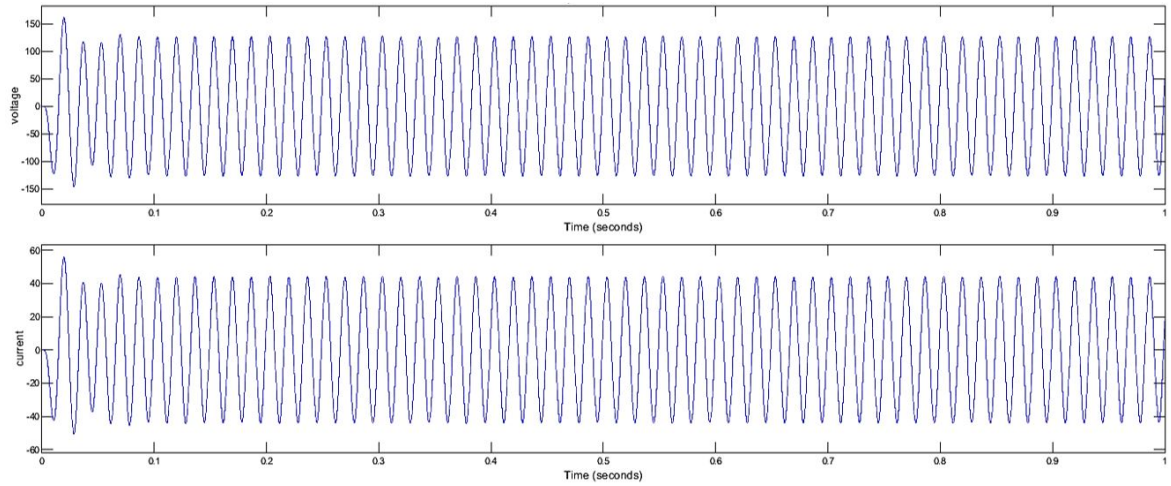

Figure 5.9: Fuzzy SMC controlled standalone mode

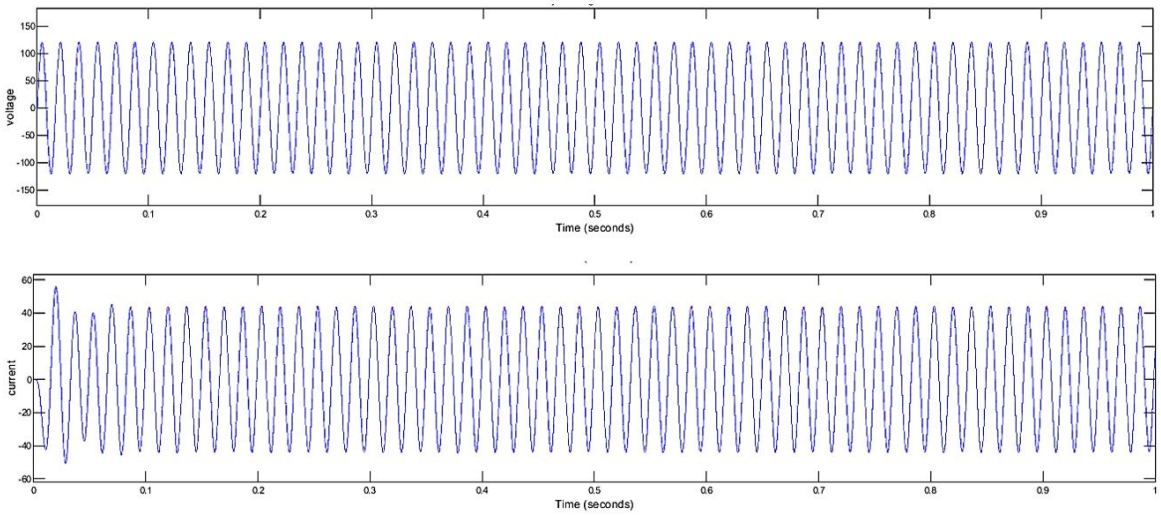

Figure 5.10: Fuzzy SMC controlled grid connected mode

5.6.1 Comparison of Results

Table 5.1: Stand alone mode

Controller	Settling Time (s)	Overshoot (%)
PI	0.15	1.85
FOPI	0.125	1.8
FPI	0.08	1.75
FSMC	0.075	1.7

Table 5.2: Grid connected mode

Controller	Settling Time (s)	Overshoot (%)
PI	0.15	2.15
FOPI	0.125	2.1
FPI	0.1	1.98
FSMC	0.08	1.8

5.7 Conclusion

This chapter covered the simulation outcomes of several controllers. These controllers' performances are examined and contrasted. It is evident that a fuzzy sliding mode controller produces superior outcomes.

Chapter 6

CONCLUSION AND FUTURE SCOPE

Here, a smart inverter with a single phase power supply is developed with energy in mind. In addition to supplying power to utility loads and local loads, SPV-SSI may inject power into the grid and store energy in Lithium Ion batteries. This work presents the full design for both a boost converter and a bi-directional buck boost converter. Additionally, fuzzy PI, fuzzy SMC, and fractional order PI controllers are used. The performance of fuzzy PI and when compared to a traditionally tuned PI controller, fuzzy SMC are more effective and reliable., demonstrating the effectiveness of the system when employing these controllers.

The future scope of the work includes analysing the controller under more voltage faults and compare with the used controllers.

References

[1] F. Blaabjerg, Z. Chen, and S. B. Kjaer, "Power electronics as efficient interface in dispersed power generation systems," *IEEE transactions on power electronics*, vol. 19, no. 5, pp. 1184–1194, 2004.

[2] K. Zeb, I. Khan, W. Uddin, M. A. Khan, P. Sathishkumar, T. D. C. Busarello, I. Ahmad, and H. Kim, "A review on recent advances and future trends of transformerless inverter structures for single-phase grid-connected photovoltaic systems," *Energies*, vol. 11, no. 8, p. 1968, 2018.

[3] F. Evran, "Plug-in repetitive control of single-phase grid-connected inverter for ac module applications," *IET Power Electronics*, vol. 10, no. 1, pp. 47–58, 2017.

[4] K. Zeb, S. U. Islam, W. Uddin, I. Khan, M. Ishfaq, T. D. C. Busarello, and H. Kim, "High-performance and multi-functional control of transformerless single-phase smart inverter for grid-connected pv system," *Journal of Modern Power Systems and Clean Energy*, vol. 9, no. 6, pp. 1386–1394, 2020.

[5] F. Fuchs, J. Dannehl, and F. Fuchs, "Discrete sliding mode current control of grid-connected three-phase pwm converters with lcl filter," in *2010 IEEE International Symposium on Industrial Electronics*, pp. 779–785, IEEE, 2010.

[6] G. Shen, X. Zhu, J. Zhang, and D. Xu, "A new feedback method for pr current control of lcl-filter-based grid-connected inverter," *IEEE Transactions on Industrial Electronics*, vol. 57, no. 6, pp. 2033–2041, 2010.

[7] K. Zeb, S. U. Islam, W. U. Din, I. Khan, M. Ishfaq, T. D. C. Busarello, I. Ahmad, and H. J. Kim, "Design of fuzzy-pi and fuzzy-sliding mode controllers for single-phase two-stages grid-connected transformerless photovoltaic inverter," *Electronics*, vol. 8, no. 5, p. 520, 2019.

[8] R. Gonzalez, J. Lopez, P. Sanchis, E. Gubia, A. Ursua, and L. Marroyo, "High-efficiency transformerless single-phase photovoltaic inverter," in *2006 12th International Power Electronics and Motion Control Conference*, pp. 1895–1900, IEEE, 2006.

[9] O. Diouri, N. Es-Sbai, F. Errahimi, A. Gaga, and C. Alaoui, "Modeling and design of single-phase pv inverter with mppt algorithm applied to the boost converter using back-stepping control in standalone mode," *International Journal of Photoenergy*, vol. 2019, 2019.

[10] W. Cui, B. Yang, Y. Zhao, W. Li, and X. He, "A novel single-phase transformerless grid-connected inverter," in *IECON 2011-37th Annual Conference of the IEEE Industrial Electronics Society*, pp. 1126–1130, IEEE, 2011.

[11] B. Gu, J. Dominic, J.-S. Lai, C.-L. Chen, T. LaBella, and B. Chen, "High reliability and efficiency single-phase transformerless inverter for grid-connected photovoltaic systems," *IEEE Transactions on Power Electronics*, vol. 28, no. 5, pp. 2235–2245, 2012.

[12] Y. Yang, K. Zhou, H. Wang, F. Blaabjerg, D. Wang, and B. Zhang, "Frequency adaptive selective harmonic control for grid-connected inverters," *IEEE Transactions on Power Electronics*, vol. 30, no. 7, pp. 3912–3924, 2014.

[13] N. Altin and İ. Sefa, "dspace based adaptive neuro-fuzzy controller of grid interactive inverter," *Energy Conversion and Management*, vol. 56, pp. 130–139, 2012.

[14] X. Fu and S. Li, "Control of single-phase grid-connected converters with lcl filters using recurrent neural network and conventional control methods," *IEEE Transactions on Power Electronics*, vol. 31, no. 7, pp. 5354–5364, 2015.

[15] N. Kamdi and P. Joshi, "Simulation of three-phase two-stage grid connected photovoltaic system using cuk converter," in *2017 Innovations in Power and Advanced Computing Technologies (i-PACT)*, pp. 1–5, IEEE, 2017.

[16] S. Salman, X. Ai, and Z. Wu, "Design of a p-&-o algorithm based mppt charge controller for a stand-alone 200w pv system," *Protection and Control of Modern Power Systems*, vol. 3, no. 1, pp. 1–8, 2018.

[17] K. S. Al-Rasheed, I. Mansy, and S. Kaddah, "Optimum operation of direct coupled photovoltaic-water pumping systems,"

[18] B. Diouf and C. Avis, "The potential of li-ion batteries in ecowas solar home systems," *Journal of Energy Storage*, vol. 22, pp. 295–301, 2019.

[19] J. Rai, N. Gupta, and P. Bansal, "Design and analysis of dc-dc boost converter," *International Journal of Advance Research and Innovation*, vol. 4, no. 3, p. 499, 2016.

[20] S. Gonzalez, F. Hoffmann, M. Mills-Price, M. Ralph, and A. Ellis, "Implementation of advanced inverter interoperability and functionality," in *2012 38th IEEE Photovoltaic Specialists Conference*, pp. 001362–001367, IEEE, 2012.

[21] K. T. Lulbadda and K. Hemapala, "The additional functions of smart inverters," *Aims Energy*, vol. 7, no. 6, pp. 971–988, 2019.

[22] O. P. Agrawal and D. Baleanu, "A hamiltonian formulation and a direct numerical scheme for fractional optimal control problems," *Journal of Vibration and Control*, vol. 13, no. 9-10, pp. 1269–1281, 2007.

[23] I. Petras, "The fractional-order controllers: Methods for their synthesis and application," *arXiv preprint math/0004064*, 2000.

[24] M. Abdelghani, E. A. Mahmoud, A. S. Abdel-Khalik, and H. F. Soliman, "An improved post-fault controller for asymmetrical six-phase induction machine using fractional order pi current controllers," in *2017 Nineteenth International Middle East Power Systems Conference (MEPCON)*, pp. 197–202, IEEE, 2017.

[25] I. Sefa, N. Altin, S. Ozdemir, and O. Kaplan, "Fuzzy pi controlled inverter for grid interactive renewable energy systems," *IET Renewable Power Generation*, vol. 9, no. 7, pp. 729–738, 2015.

[26] A. Sözen, E. Arcaklioğlu, A. Erisen, and M. A. Akçayol, "Performance prediction of a vapour-compression heat-pump," *Applied energy*, vol. 79, no. 3, pp. 327–344, 2004.

[27] I. Khan, K. Zeb, W. U. Din, S. U. Islam, M. Ishfaq, S. Hussain, and H.-J. Kim, "Dynamic modeling and robust controllers design for doubly fed induction generator-based wind turbines under unbalanced grid fault conditions," *Energies*, vol. 12, no. 3, p. 454, 2019.

[28] K. Zeb, M. S. Nazir, I. Ahmad, W. Uddin, and H.-J. Kim, "Control of transformerless inverter-based two-stage grid-connected photovoltaic system using adaptive-pi and adaptive sliding mode controllers," *Energies*, vol. 14, no. 9, p. 2546, 2021.

[29] K. Zeb, W. U. Din, M. A. Khan, A. Khan, U. Younas, T. D. C. Busarello, and H. J. Kim, "Dynamic simulations of adaptive design approaches to control the speed of an induction machine considering parameter uncertainties and external perturbations," *Energies*, vol. 11, no. 9, p. 2339, 2018.

List of Publications

[1] Risana S and Irfan Habeeb, "Control of Transformerless Inverter for a PV System using Fuzzy Logic and Fractional Controller," communicated to *International Conference on Electrical Engineering and Control Technologies (ICEECT)*, 2022.